PML absorbing boundary condition for non-linear aeroacoustics problems

Fang Q. Hu^{*}, X. D. Li[†] and D. K. Lin[‡]

*Old Dominion University, Norfolk, Virginia 23529, USA

† Beihang University, Xueyuan Road 37, Beijing 100083, P. R. China

Perfectly Matched Layer (PML) absorbing boundary condition for the compressible non-linear Navier-Stokes equation is derived. It follows the essential steps used in the derivation of PML for the non-linear Euler equation which is now a special case of the current PML formulation. The PML is also given in the conservation form for its easy implementation in most existing codes in Computational Aeroacoustics and Computational Fluid Dynamics. Numerical examples of a viscous vortex transport and vortex shedding from a viscous flow over a circular cylinder are presented. Satisfactory results demonstrated that the proposed PML absorbing boundary condition is highly accurate, effective and numerically stable for non-linear viscous flow problems.

I. Introduction

Perfectly Matched Layer (PML) is a recently emerged technique for developing non-reflecting boundary conditions. The significance of PML technique lies in the fact that the absorbing zone is theoretically reflectionless for multi-dimensional linear waves of any angle and frequency.^{3,8} Substantial progress has been made in the past few years on the development of PML technique for the Euler equations that is highly accurate, effective and numerically stable.^{1,4-6,10,11} Although the PML technique itself is rather simple when it is viewed as a complex change of variable in the frequency domain, it has now been recognized that, for the PML technique to yield dynamically stable absorbing boundary conditions, the phase and group velocities of the physical waves supported by the governing equations must be consistent and in the same direction.^{2,4,10} For governing equations that support physical waves that have inconsistent phase and group velocities, such as the Euler equations for fluid dynamics, a space-time transformation may be utilized before applying the

^{*}Professor, Department of Mathematics and Statistics, Senior member AIAA

[†]Professor, School of Jet Propulsion, Senior member AIAA

[‡]Graduate student, School of Jet Propulsion

Copyright © 2006 by the American Institute of Aeronautics and Astronautics. All rights reserved.

PML technique in the derivation process.^{10,11} This space-time transformation corrects the inconsistency in the phase and group velocities. An emerging method of formulating PML involves essentially three steps:¹³

- 1. A proper space-time transformation is determined and applied to the governing equations;
- 2. A PML complex change of variable is applied in the frequency domain;
- 3. The time domain absorbing boundary condition is derived from the frequency domain equation.

This procedure has been successfully applied to the linearized Euler equations with a mean flow aligned with a spatial axis^{10,11} and, most recently, to the non-linear Euler equations in [12].

In the present paper, further application of the PML technique to the non-linear Navier-Stokes equation is considered. Derivation of the PML equations is given by applying the three steps outlined above to the non-linear Navier-Stokes equation in conservation form. With increased order in spatial derivatives due to viscous effects, the extension of PML technique will now result in more auxiliary variables in the PML domain. For convenience of implementation of PML in most existing codes, all the PML equations are formulated in conservation form. In the next section, the details on the construction of time-domain PML equation are given. Numerical examples are presented in section III.

II. Derivation of PML equations for non-linear Navier-Stokes equation

At non-reflecting boundaries, we introduce PML domains to absorb out-going disturbances, as shown in Figure 1. We wish to formulate the equations to be used in the PML domains so that out-going waves can be exponentially reduced once they enter the added zones while causing as little numerical reflection as possible.

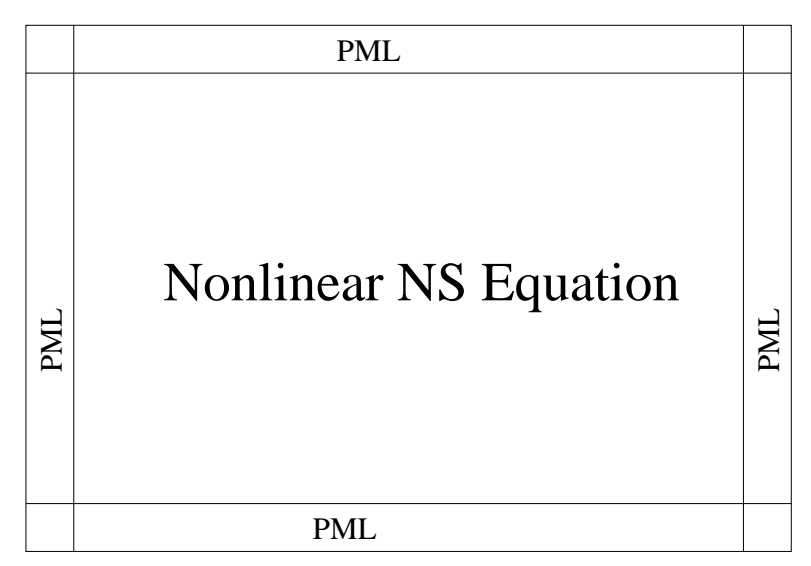


Figure 1. Schematics of physical and PML domains.

We consider the compressible non-linear Navier-Stokes equation written in the conservation form as

$$\frac{\partial \mathbf{u}}{\partial t} + \frac{\partial \mathbf{F}_1(\mathbf{u})}{\partial x} + \frac{\partial \mathbf{F}_2(\mathbf{u})}{\partial y} = 0 \tag{1}$$

where

$$\mathbf{u} = \begin{bmatrix} \rho \\ \rho u \\ \rho v \\ \rho e \end{bmatrix} \tag{2}$$

$$\mathbf{F}_{1}(\mathbf{u}) = \begin{vmatrix} \rho u \\ \rho u^{2} + p - \tau_{xx} \\ \rho uv - \tau_{xy} \\ (\rho e + p)u - u\tau_{xx} - v\tau_{xy} + q_{x} \end{vmatrix}$$
(3)

$$\mathbf{F}_{2}(\mathbf{u}) = \begin{bmatrix} \rho v \\ \rho uv - \tau_{xy} \\ \rho v^{2} + p - \tau_{yy} \\ (\rho e + p)v - u\tau_{yx} - v\tau_{yy} + q_{y} \end{bmatrix}$$

$$(4)$$

and

$$\tau_{xx} = \frac{M}{Re} \left(\frac{4}{3} \frac{\partial u}{\partial x} - \frac{2}{3} \frac{\partial v}{\partial y} \right), \quad \tau_{xy} = \frac{M}{Re} \left(\frac{\partial u}{\partial y} + \frac{\partial v}{\partial x} \right), \quad \tau_{yy} = \frac{M}{Re} \left(\frac{4}{3} \frac{\partial v}{\partial y} - \frac{2}{3} \frac{\partial u}{\partial x} \right)$$
 (5)

$$q_x = -\frac{M}{(\gamma - 1)PrRe} \frac{\partial T}{\partial x}, \quad q_y = -\frac{M}{(\gamma - 1)PrRe} \frac{\partial T}{\partial y}$$
 (6)

and

$$\gamma p = \rho T, \ e = \frac{u^2 + v^2}{2} + \frac{p}{(\gamma - 1)\rho}$$
 (7)

In the above, u and v are the velocity components, p is the pressure, ρ is the density, T is the temperature and e is the energy. The velocity is non-dimensionalized by a reference speed of sound a_{∞} , density by ρ_{∞} and pressure by $\rho_{\infty}a_{\infty}^2$. Also Re is the Reynolds number based on a characteristic flow velocity U_{∞} and M is the Mach number U_{∞}/a_{∞} . Pr is the Prandtl number and γ is the specific heats ratio.

To facilitate the derivation of PML equations for (1), we introduce

$$\mathbf{G}(\mathbf{u}) = \begin{bmatrix} u \\ v \\ T \end{bmatrix},\tag{8}$$

and new unknowns

$$\mathbf{e}_{1} = \frac{\partial \mathbf{G}(\mathbf{u})}{\partial x} \equiv \begin{bmatrix} \frac{\partial u}{\partial x} \\ \frac{\partial v}{\partial x} \\ \frac{\partial T}{\partial x} \end{bmatrix}, \quad \mathbf{e}_{2} = \frac{\partial \mathbf{G}(\mathbf{u})}{\partial y} \equiv \begin{bmatrix} \frac{\partial u}{\partial y} \\ \frac{\partial v}{\partial y} \\ \frac{\partial T}{\partial y} \end{bmatrix}$$
(9)

Then, we can re-define the flux vectors \mathbf{F}_1 and \mathbf{F}_2 of (3) and (4) as functions of \mathbf{u} , \mathbf{e}_1 and \mathbf{e}_2 , and re-write (1) as

$$\frac{\partial \mathbf{u}}{\partial t} + \frac{\partial \mathbf{F}_1(\mathbf{u}, \mathbf{e}_1, \mathbf{e}_2)}{\partial x} + \frac{\partial \mathbf{F}_2(\mathbf{u}, \mathbf{e}_1, \mathbf{e}_2)}{\partial y} = 0$$
(10)

Equations (10) and (9) form a system of equations for unknowns \mathbf{u} , \mathbf{e}_1 and \mathbf{e}_2 . This system is only a re-writing of the original Navier-Stokes equation (1) and thus is equivalent to (1). We note that now $\mathbf{F}_1(\mathbf{u}, \mathbf{e}_1, \mathbf{e}_2)$ and $\mathbf{F}_2(\mathbf{u}, \mathbf{e}_1, \mathbf{e}_2)$ do not involve explicitly the spatial second derivatives of \mathbf{u} . In what follows, we shall derive the PML equations for (10) and (9).

In a non-linear simulation, a solution of equation (1) can be considered as consisting of a time independent mean-state and a perturbation that has to be governed by non-linear equations. Since the mean-state could be large compared to the time-dependent perturbed state, as pointed out in [12], it may not be most efficient to absorb the total variable \mathbf{u} and to reduce it to nearly zero inside the PML domain. Although it is common to decompose the total variable \mathbf{u} into a time-independent mean-flow and a time-dependent fluctuation, the exact mean-state is usually unknown at the start of the computation. The PML formulation presented here will not require the exact mean-flow. Instead, following [12], we shall partition the solution inside the PML domain into two parts as

$$\mathbf{u} = \bar{\mathbf{u}}_p + \mathbf{u}', \ \mathbf{e}_1 = \bar{\mathbf{e}}_1 + \mathbf{e}_1', \ \mathbf{e}_2 = \bar{\mathbf{e}}_2 + \mathbf{e}_2'$$
 (11)

with

$$\bar{\mathbf{e}}_1 = \frac{\partial \mathbf{G}(\bar{\mathbf{u}}_p)}{\partial x}, \ \bar{\mathbf{e}}_2 = \frac{\partial \mathbf{G}(\bar{\mathbf{u}}_p)}{\partial y}$$
(12)

where $\bar{\mathbf{u}}_p$ is a time-independent "pseudo mean-flow".^{9,12} We only require that the chosen $\bar{\mathbf{u}}_p$ satisfy the steady-state Navier-Stokes equation:

$$\frac{\partial \mathbf{F}_1(\bar{\mathbf{u}}_p, \bar{\mathbf{e}}_1, \bar{\mathbf{e}}_2)}{\partial x} + \frac{\partial \mathbf{F}_2(\bar{\mathbf{u}}_p, \bar{\mathbf{e}}_1, \bar{\mathbf{e}}_2)}{\partial y} = 0$$
(13)

It is important to emphasize that it is not necessary for this pseudo mean-flow to be the exact mean-flow at the non-reflecting boundary. The use of $\bar{\mathbf{u}}_p$ is only to make the PML domain more efficient since we now need only to absorb \mathbf{u}' , \mathbf{e}'_1 and \mathbf{e}'_2 , the differences between total flow variables and that of a prescribed pseudo mean-flow. It also follows that the choice for $\bar{\mathbf{u}}_p$ is not unique.¹²

Using (11)-(13), the equations for \mathbf{u}' , \mathbf{e}'_1 and \mathbf{e}'_2 become

$$\frac{\partial \mathbf{u}'}{\partial t} + \frac{\partial [\mathbf{F}_1(\mathbf{u}, \mathbf{e}_1, \mathbf{e}_2) - \mathbf{F}_1(\bar{\mathbf{u}}_p, \bar{\mathbf{e}}_1, \bar{\mathbf{e}}_2)]}{\partial x} + \frac{\partial [\mathbf{F}_2(\mathbf{u}, \mathbf{e}_1, \mathbf{e}_2) - \mathbf{F}_2(\bar{\mathbf{u}}_p, \bar{\mathbf{e}}_1, \bar{\mathbf{e}}_2)]}{\partial y} = 0$$
(14)

$$\mathbf{e}_{1}' = \frac{\partial [\mathbf{G}(\mathbf{u}) - \mathbf{G}(\bar{\mathbf{u}}_{p})]}{\partial x}, \ \mathbf{e}_{2}' = \frac{\partial [\mathbf{G}(\mathbf{u}) - \mathbf{G}(\bar{\mathbf{u}}_{p})]}{\partial y}$$
(15)

We shall now derive the PML equations that absorb \mathbf{u}' , \mathbf{e}'_1 and \mathbf{e}'_2 .

Following the three-step method for the derivation of PML described in Introduction, we first apply a spacetime transformation of the form

$$\bar{t} = t + \beta x$$
,

to equations (14)-(15) and get

$$\frac{\partial \mathbf{u}'}{\partial \bar{t}} + \beta \frac{\partial [\mathbf{F}_{1}(\mathbf{u}, \mathbf{e}_{1}, \mathbf{e}_{2}) - \mathbf{F}_{1}(\bar{\mathbf{u}}_{p}, \bar{\mathbf{e}}_{1}, \bar{\mathbf{e}}_{2})]}{\partial \bar{t}} + \frac{\partial [\mathbf{F}_{1}(\mathbf{u}, \mathbf{e}_{1}, \mathbf{e}_{2}) - \mathbf{F}_{1}(\bar{\mathbf{u}}_{p}, \bar{\mathbf{e}}_{1}, \bar{\mathbf{e}}_{2})]}{\partial x} + \frac{\partial [\mathbf{F}_{2}(\mathbf{u}, \mathbf{e}_{1}, \mathbf{e}_{2}) - \mathbf{F}_{2}(\bar{\mathbf{u}}_{p}, \bar{\mathbf{e}}_{1}, \bar{\mathbf{e}}_{2})]}{\partial y} = 0$$
 (16)

$$\mathbf{e}_{1}' = \beta \frac{\partial [\mathbf{G}(\mathbf{u}) - \mathbf{G}(\bar{\mathbf{u}}_{p})]}{\partial \bar{t}} + \frac{\partial [\mathbf{G}(\mathbf{u}) - \mathbf{G}(\bar{\mathbf{u}}_{p})]}{\partial x}, \quad \mathbf{e}_{2}' = \frac{\partial [\mathbf{G}(\mathbf{u}) - \mathbf{G}(\bar{\mathbf{u}}_{p})]}{\partial y}$$
(17)

Here, parameter β is determined from the linear dispersive wave analysis of the pseudo mean-flow as described in detail in [11] and [12]. This transformation is necessary to maintain the linear stability of the PML equations. In frequency domain, the above is

$$(-i\bar{\omega}\tilde{\mathbf{u}}') + \beta(-i\bar{\omega})[\mathbf{F}_{1}(\mathbf{u},\mathbf{e}_{1},\mathbf{e}_{2}) - \mathbf{F}_{1}(\bar{\mathbf{u}}_{p},\bar{\mathbf{e}}_{1},\bar{\mathbf{e}}_{2})] + \frac{\partial[\mathbf{F}_{1}(\mathbf{u},\mathbf{e}_{1},\mathbf{e}_{2}) - \mathbf{F}_{1}(\bar{\mathbf{u}}_{p},\bar{\mathbf{e}}_{1},\bar{\mathbf{e}}_{2})]}{\partial x} + \frac{\partial[\mathbf{F}_{2}(\mathbf{u},\mathbf{e}_{1},\mathbf{e}_{2}) - \mathbf{F}_{2}(\bar{\mathbf{u}}_{p},\bar{\mathbf{e}}_{1},\bar{\mathbf{e}}_{2})]}{\partial y} = 0$$

$$(18)$$

$$\tilde{\mathbf{e}}_{1}' = \beta(-i\bar{\omega})[\mathbf{G}(\mathbf{u}) - \mathbf{G}(\bar{\mathbf{u}}_{p})] + \frac{\partial[\mathbf{G}(\mathbf{u}) - \mathbf{G}(\bar{\mathbf{u}}_{p})]}{\partial x}, \quad \mathbf{e}_{2}' = \frac{\partial[\mathbf{G}(\mathbf{u}) - \mathbf{G}(\bar{\mathbf{u}}_{p})]}{\partial y}$$
(19)

where an over tilde indicates the time Fourier-transformed variable

In the second step, we apply the PML complex change of variables to (18) and (19), i.e., we modify the spatial derivatives as¹¹

$$\frac{\partial}{\partial x} \to \frac{1}{1+i\frac{\sigma_x}{G}}\frac{\partial}{\partial x}, \quad \frac{\partial}{\partial y} \to \frac{1}{1+i\frac{\sigma_y}{G}}\frac{\partial}{\partial y}$$

where σ_x and σ_y are absorption coefficients and are positive functions of x and y respectively. Then, the PML equations for (18)-(19) in the frequency domain are

$$(-i\bar{\omega}\tilde{\mathbf{u}}') + \beta(-i\bar{\omega})[\mathbf{F}_{1}(\mathbf{u},\mathbf{e}_{1},\mathbf{e}_{2}) - \mathbf{F}_{1}(\bar{\mathbf{u}}_{p},\bar{\mathbf{e}}_{1},\bar{\mathbf{e}}_{2})] + \frac{1}{1 + \frac{i\sigma_{x}}{\bar{\omega}}} \frac{\partial[\mathbf{F}_{1}(\mathbf{u},\mathbf{e}_{1},\mathbf{e}_{2}) - \mathbf{F}_{1}(\bar{\mathbf{u}}_{p},\bar{\mathbf{e}}_{1},\bar{\mathbf{e}}_{2})]}{\partial x}$$

$$+\frac{1}{1+\frac{i\sigma_y}{\bar{\mathbf{q}}}}\frac{\partial [\mathbf{F}_2(\mathbf{u},\mathbf{e}_1,\mathbf{e}_2) - \mathbf{F}_2(\bar{\mathbf{u}}_p,\bar{\mathbf{e}}_1,\bar{\mathbf{e}}_2)]}{\partial y} = 0$$
 (20)

$$\tilde{\mathbf{e}}_{1}' = \beta(-i\bar{\omega})[\mathbf{G}(\mathbf{u}) - \mathbf{G}(\bar{\mathbf{u}}_{p})] + \frac{1}{1 + \frac{i\sigma_{x}}{\bar{\omega}}} \frac{\partial[\mathbf{G}(\mathbf{u}) - \mathbf{G}(\bar{\mathbf{u}}_{p})]}{\partial x}$$
(21)

$$\tilde{\mathbf{e}}_{2}' = \frac{1}{1 + \frac{i\sigma_{y}}{\bar{\omega}}} \frac{\partial [\mathbf{G}(\mathbf{u}) - \mathbf{G}(\bar{\mathbf{u}}_{p})]}{\partial y}$$
(22)

Finally, to write the above in the time domain, we use the split approach of [12]. We first split (20) and re-write it as two equations,

$$(-i\bar{\omega}\tilde{\mathbf{u}}_{1}') + \beta(-i\bar{\omega})[\mathbf{F}_{1}(\mathbf{u}, \mathbf{e}_{1}, \mathbf{e}_{2}) - \mathbf{F}_{1}(\bar{\mathbf{u}}_{p}, \bar{\mathbf{e}}_{1}, \bar{\mathbf{e}}_{2})] + \frac{1}{1 + \frac{i\sigma_{x}}{\bar{\omega}}} \frac{\partial[\mathbf{F}_{1}(\mathbf{u}, \mathbf{e}_{1}, \mathbf{e}_{2}) - \mathbf{F}_{1}(\bar{\mathbf{u}}_{p}, \bar{\mathbf{e}}_{1}, \bar{\mathbf{e}}_{2})]}{\partial x} = 0$$
 (23)

$$(-i\bar{\omega}\tilde{\mathbf{u}}_{2}') + \frac{1}{1 + \frac{i\sigma_{y}}{\bar{\omega}}} \frac{\partial [\mathbf{F}_{2}(\mathbf{u}, \mathbf{e}_{1}, \mathbf{e}_{2}) - \mathbf{F}_{2}(\bar{\mathbf{u}}_{p}, \bar{\mathbf{e}}_{1}, \bar{\mathbf{e}}_{2})]}{\partial y} = 0$$
(24)

where

$$\tilde{\mathbf{u}}' = \tilde{\mathbf{u}}_1' + \tilde{\mathbf{u}}_2'$$

By multiplying $(1 + \frac{i\sigma_x}{\bar{\omega}})$ to (23) and (21), and multiplying $(1 + \frac{i\sigma_y}{\bar{\omega}})$ to (24) and (22), we get the following set of equations,

$$(-i\bar{\omega} + \sigma_x)\tilde{\mathbf{u}}_1' + \beta(-i\bar{\omega} + \sigma_x)[\mathbf{F}_1(\mathbf{u}, \mathbf{e}_1, \mathbf{e}_2) - \mathbf{F}_1(\bar{\mathbf{u}}_p, \bar{\mathbf{e}}_1, \bar{\mathbf{e}}_2)] + \frac{\partial[\mathbf{F}_1(\mathbf{u}, \mathbf{e}_1, \mathbf{e}_2) - \mathbf{F}_1(\bar{\mathbf{u}}_p, \bar{\mathbf{e}}_1, \bar{\mathbf{e}}_2)]}{\partial x} = 0$$
(25)

$$(-i\bar{\omega} + \sigma_y)\tilde{\mathbf{u}}_2' + \frac{\partial [\mathbf{F}_2(\mathbf{u}, \mathbf{e}_1, \mathbf{e}_2) - \mathbf{F}_2(\bar{\mathbf{u}}_p, \bar{\mathbf{e}}_1, \bar{\mathbf{e}}_2)]}{\partial y} = 0$$
(26)

$$(1 + \frac{i\sigma_x}{\bar{\omega}})\tilde{\mathbf{e}}_1' = \beta(-i\bar{\omega} + \sigma_x)[\mathbf{G}(\mathbf{u}) - \mathbf{G}(\bar{\mathbf{u}}_p)] + \frac{\partial[\mathbf{G}(\mathbf{u}) - \mathbf{G}(\bar{\mathbf{u}}_p)]}{\partial x}$$
(27)

$$(1 + \frac{i\sigma_y}{\bar{\omega}})\mathbf{e}_2' = \frac{\partial [\mathbf{G}(\mathbf{u}) - \mathbf{G}(\bar{\mathbf{u}}_p)]}{\partial y}$$
(28)

It is easy to find the correspondent time domain equations for (25)-(28). Following similar steps in [12], we get the time-domain PML equations in the original physical space and time variables as follows,

$$\frac{\partial \mathbf{u}_{1}'}{\partial t} + \sigma_{x}\mathbf{u}_{1}' + \beta\sigma_{x}[\mathbf{F}_{1}(\mathbf{u}, \mathbf{e}_{1}, \mathbf{e}_{2}) - \mathbf{F}_{1}(\bar{\mathbf{u}}_{p}, \bar{\mathbf{e}}_{1}, \bar{\mathbf{e}}_{2})] + \frac{\partial [\mathbf{F}_{1}(\mathbf{u}, \mathbf{e}_{1}, \mathbf{e}_{2}) - \mathbf{F}_{1}(\bar{\mathbf{u}}_{p}, \bar{\mathbf{e}}_{1}, \bar{\mathbf{e}}_{2})]}{\partial x} = 0$$
(29)

$$\frac{\partial \mathbf{u}_2'}{\partial t} + \sigma_y \mathbf{u}_2' + \frac{\partial [\mathbf{F}_2(\mathbf{u}, \mathbf{e}_1, \mathbf{e}_2) - \mathbf{F}_2(\bar{\mathbf{u}}_p, \bar{\mathbf{e}}_1, \bar{\mathbf{e}}_2)]}{\partial y} = 0$$
(30)

$$\mathbf{e}_{1}' + \sigma_{x}\mathbf{q}_{1} = \beta\sigma_{x}[\mathbf{G}(\mathbf{u}) - \mathbf{G}(\bar{\mathbf{u}}_{p})] + \frac{\partial[\mathbf{G}(\mathbf{u}) - \mathbf{G}(\bar{\mathbf{u}}_{p})]}{\partial x}$$
(31)

$$\mathbf{e}_{2}' + \sigma_{y}\mathbf{q}_{2} = \frac{\partial[\mathbf{G}(\mathbf{u}) - \mathbf{G}(\bar{\mathbf{u}}_{p})]}{\partial y}$$
(32)

$$\frac{\partial \mathbf{q}_1}{\partial t} = \mathbf{e}_1' \tag{33}$$

$$\frac{\partial \mathbf{q}_2}{\partial t} = \mathbf{e}_2' \tag{34}$$

in which \mathbf{q}_1 and \mathbf{q}_2 are auxiliary variables introduced for the time-domain equations of \mathbf{e}'_1 and \mathbf{e}'_2 respectively.

Finally, equations (23)-(34) can be re-arranged into a form that is easy to implement in time marching schemes, and we write the PML equations in the following form,

$$\frac{\partial \mathbf{u}}{\partial t} + \frac{\partial [\mathbf{F}_{1}(\mathbf{u}, \mathbf{e}_{1}, \mathbf{e}_{2}) - \mathbf{F}_{1}(\bar{\mathbf{u}}_{p}, \bar{\mathbf{e}}_{1}, \bar{\mathbf{e}}_{2})]}{\partial x} + \frac{\partial [\mathbf{F}_{2}(\mathbf{u}, \mathbf{e}_{1}, \mathbf{e}_{2}) - \mathbf{F}_{2}(\bar{\mathbf{u}}_{p}, \bar{\mathbf{e}}_{1}, \bar{\mathbf{e}}_{2})]}{\partial y} + \sigma_{x}(\mathbf{u} - \bar{\mathbf{u}}_{p} - \mathbf{q}) + \sigma_{y}\mathbf{q} + \beta\sigma_{x}[\mathbf{F}_{1}(\mathbf{u}, \mathbf{e}_{1}, \mathbf{e}_{2}) - \mathbf{F}_{1}(\bar{\mathbf{u}}_{p}, \bar{\mathbf{e}}_{1}, \bar{\mathbf{e}}_{2})] = 0$$
(35)

$$\frac{\partial \mathbf{q}}{\partial t} + \sigma_y \mathbf{q} + \frac{\partial [\mathbf{F}_2(\mathbf{u}, \mathbf{e}_1, \mathbf{e}_2) - \mathbf{F}_2(\bar{\mathbf{u}}_p, \bar{\mathbf{e}}_1, \bar{\mathbf{e}}_2)]}{\partial y} = 0$$
(36)

$$\frac{\partial \mathbf{q}_1}{\partial t} + \sigma_x \mathbf{q}_1 = \frac{\partial [\mathbf{G}(\mathbf{u}) - \mathbf{G}(\bar{\mathbf{u}}_p)]}{\partial x} + \beta \sigma_x [\mathbf{G}(\mathbf{u}) - \mathbf{G}(\bar{\mathbf{u}}_p)]$$
(37)

$$\frac{\partial \mathbf{q}_2}{\partial t} + \sigma_y \mathbf{q}_2 = \frac{\partial [\mathbf{G}(\mathbf{u}) - \mathbf{G}(\bar{\mathbf{u}}_p)]}{\partial y}$$
(38)

where

$$\mathbf{e}_{1} = \frac{\partial \mathbf{G}(\mathbf{u})}{\partial x} - \sigma_{x} \mathbf{q}_{1} + \beta \sigma_{x} [\mathbf{G}(\mathbf{u}) - \mathbf{G}(\bar{\mathbf{u}}_{p})]$$
(39)

$$\mathbf{e}_2 = \frac{\partial \mathbf{G}(\mathbf{u})}{\partial y} - \sigma_y \mathbf{q}_2 \tag{40}$$

We note first that the PML equations given above, (35)-(40), include the PML for the inviscid non-linear Euler equation as a special case. Equations (35) and (36) are identical to the PML for the Euler equation given in ref¹² when the viscous terms involving \mathbf{e}_1 and \mathbf{e}_2 are ignored.

Second, although we have required that the pseudo mean-flow satisfy the steady-state Navier-State equation (13) in the derivation, the PML equations as given by (35)-(38) are still consistent in the limit of $\mathbf{u} \to \bar{\mathbf{u}}_p$ even if $\bar{\mathbf{u}}_p$, $\bar{\mathbf{e}}_1$ and $\bar{\mathbf{e}}_2$ do not exactly satisfy (13).

III. Numerical examples

In this section, we present numerical examples of using PML as the non-reflecting boundary conditions for the non-linear Navier-Stokes equation based on a viscous computational aeroacoustic approach 15 . The dispersion-relation-preserving scheme 18 is applied for spatial discretization and the optimized 5- and 6-stage alternating low-dissipation and low-dispersion Runge-Kutta scheme 14 is used for time integration.

A. Convection of a vortex

In this example, we consider an advective vortex which is an exact solution of the non-linear Euler equation,

$$\begin{pmatrix} \rho(\mathbf{x},t) \\ u(\mathbf{x},t) \\ v(\mathbf{x},t) \\ p(\mathbf{x},t) \end{pmatrix} = \begin{pmatrix} 0 \\ U_0 \\ V_0 \\ 0 \end{pmatrix} + \begin{pmatrix} \rho_r(r) \\ -u_r(r)\sin\theta \\ u_r(r)\cos\theta \\ p_r(r) \end{pmatrix}$$
(41)

where $r = \sqrt{(x - U_0 t)^2 + (y - V_0 t)^2}$ and, for any given $u_r(r)$ and $\rho_r(r)$, the pressure $p_r(r)$ is found by

$$\frac{d}{dr}p_r(r) = \rho_r(r)\frac{u_r^2(r)}{r} \tag{42}$$

For isentropic flow, we assume

$$p_r = \frac{1}{\gamma} \rho_r^{\gamma} \tag{43}$$

and, by integrating (42), we get the following density and pressure distributions,

$$\rho_r(r) = \left(1 - \frac{1}{2}(\gamma - 1)U_{max}^{\prime 2}e^{1 - \frac{r^2}{b^2}}\right)^{1/(\gamma - 1)}$$
(44)

$$p_r(r) = \frac{1}{\gamma} \left(1 - \frac{1}{2} (\gamma - 1) U_{max}^{\prime 2} e^{1 - \frac{r^2}{b^2}} \right)^{\gamma/(\gamma - 1)}$$
(45)

When viscosity is ignored, equation (41) gives a solution that advects with constant velocity (U_0, V_0) .

For our numerical tests, we consider a velocity distribution of the form

$$u_r(r) = \frac{U'_{max}}{b} r e^{\frac{1}{2}(1 - \frac{r^2}{b^2})} \tag{46}$$

where U'_{max} is the maximum velocity at r=b. This example has been used in [12] in testing the PML for the non-linear Euler equation. Here we will show the numerical solution of the non-linear Navier-Stokes equation (1) with initial condition given by (41). Equations (35)-(38) are used in the PML absorbing zones that surround the physical domain. A numerical solution is shown in Figure 2. The Reynolds number, based on the mean-flow velocity U_0 , is Re=500 and the initial condition is that given in (41) with $(U_0, V_0)=(0.5, 0)$ and $U'_{max}=0.25$, b=0.2. Pr=0.712. The non-linear Navier-Stokes equation (1) is solved using a computational domain $[-1.2, 1.2] \times [-1.2, 1.2]$ with $\Delta x=\Delta y=0.02$, including the surrounding PML domain of width 10 grid points. The pseudo mean-flow is the same as the uniform background flow with parameter $\beta = U_0/(1-U_0^2)$. In particular, the PML absorption coefficient

$$\sigma_x = \sigma_{max} \left| \frac{x - x_0}{D} \right|^{\alpha}$$

with $\sigma_{max} = 20$, $\alpha = 4$ and similar model for σ_y is used. A grid stretching in the PML domain is also used to increase the efficiency of the absorbing zone.^{17,19} The stretching factor is

$$\alpha(x) = 1 + 2 \left| \frac{x - x_0}{D} \right|^2$$

To assess the reflection error, Figure 3 plots the maximum difference between the numerical solution and a reference solution obtained using a larger computational domain, along a vertical line near the outflow boundary, as a function of time. The reflection errors are indeed quite small and reduces with an increase in the width of the PML domain employed.

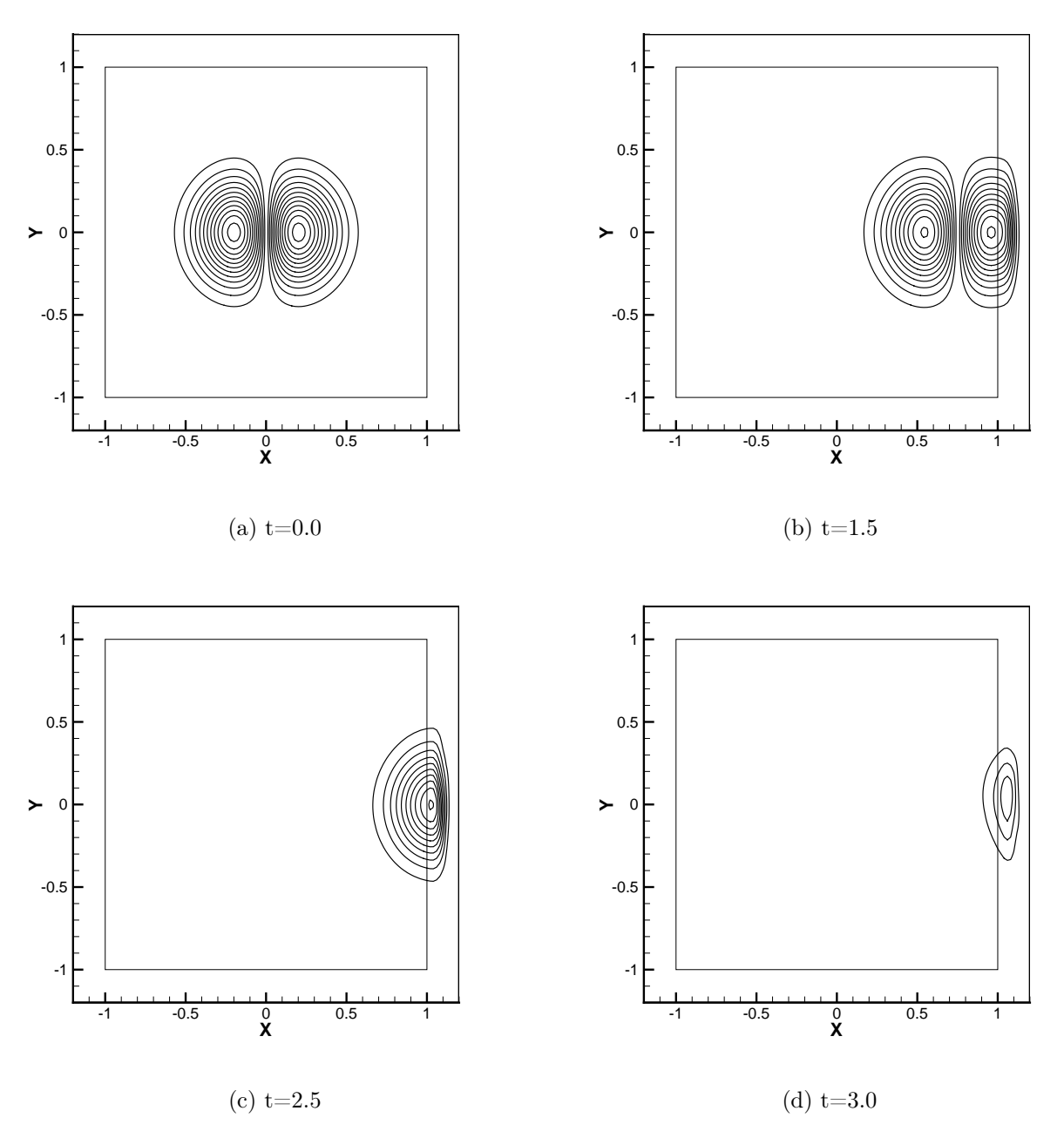


Figure 2. v-velocity contour levels from ± 0.02 to ± 0.24 . Re=500

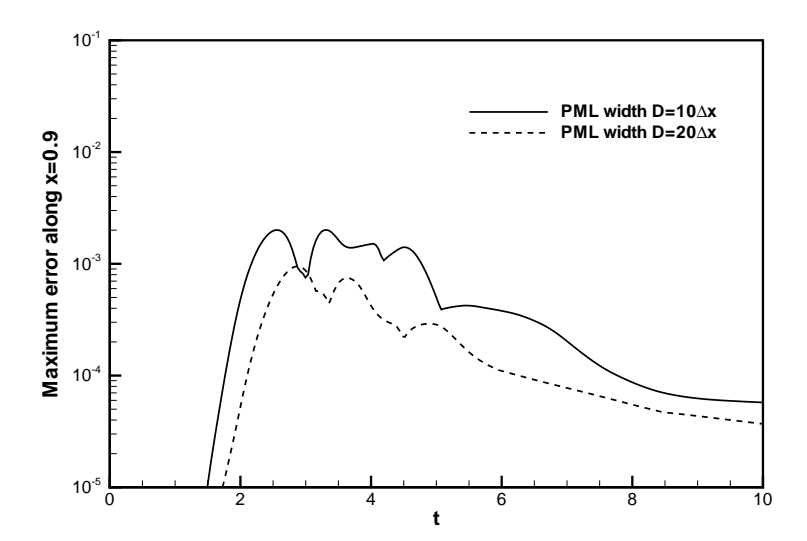


Figure 3. Maximum reflection error (v-velocity component) relative to the maximum vortex velocity U'_{max} along x=0.9. PML width D is as indicated

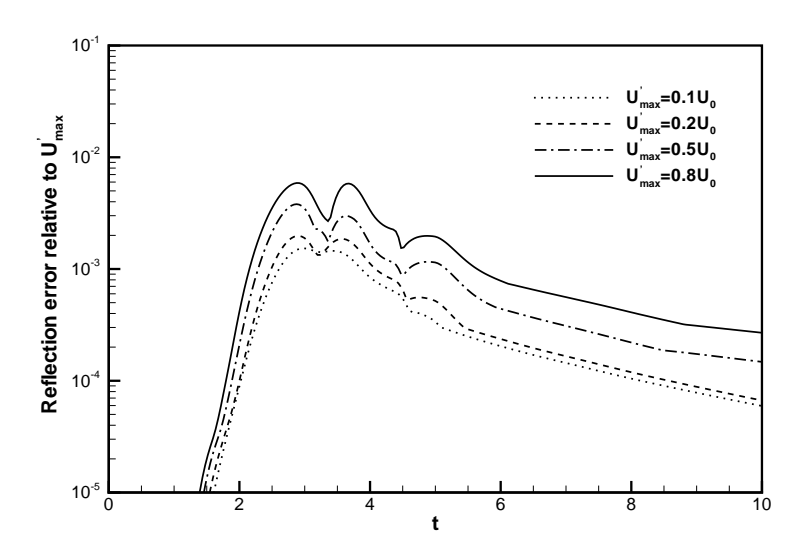


Figure 4. Maximum reflection error (v-velocity component) along x=0.9. PML width $D=20\Delta x$

Figure 4 shows the maximum reflection error relative to the maximum velocity of the vortex along x = 0.9 near the outflow boundary for various strengths of the vortex. Although reflection error generally increases with an increase in the strength of the vortex, the maximum relative error is less than 0.6% for all the cases with a PML width of 20 grid points.

B. Viscous flow over a circular cylinder

In this example, we show the absorption of non-linear vortices shedded by a viscous flow over a circular cylinder. The uniform incoming flow has a Mach number $M=U_{\infty}/a_{\infty}=0.2$. Here U_{∞} and a_{∞} denote the velocity of the uniform flow and the speed of sound respectively. The velocity and the lengths are nondimensionalize by a_{∞} and d respectively, where d is the diameter of the cylinder. The Reynolds number is defined as $Re=U_{\infty}d/\nu_{\infty}$, where ν_{∞} is the kinematic viscosity. For this case Re=150, and the Prandtl number Pr=0.75, and the ratio of specific heats is 1.4.

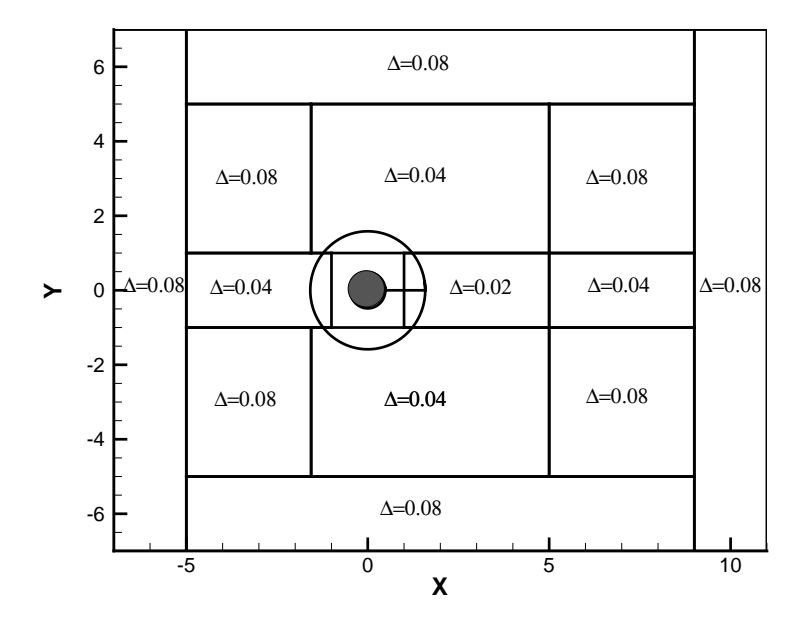


Figure 5. Mesh and computational domain (global)

Figure 5 and Figure 6 show the multi-domain computational mesh layout with overset grids, for $(x,y) \in [-7,11] \times [-7,7]$. The cylinder is located at (x,y)=(0,0) with a radius of 0.5 and all PML domains have a width of 20 grid points. The computational domain is divided into two regions. An O-grid system with non-uniform meshes is adopted around the cylinder, covering a region of $0.5 \le r \le 1.5, 0 \le \theta \le 2\pi$, with $\Delta r_{min} = 0.005, \Delta r_{max} = 0.02, \Delta \theta = 1.2^{\circ}$. Another region is composed of multi-block uniform meshes with $\Delta x = \Delta y = \Delta$ in each block, and the values of Δ are specified as shown in Figure 5. A high-order Lagrange interpolation technique is utilized for overset grids. ¹⁶

Calculation is initiated with the uniform flow for the entire computational domain. A natural choice for the

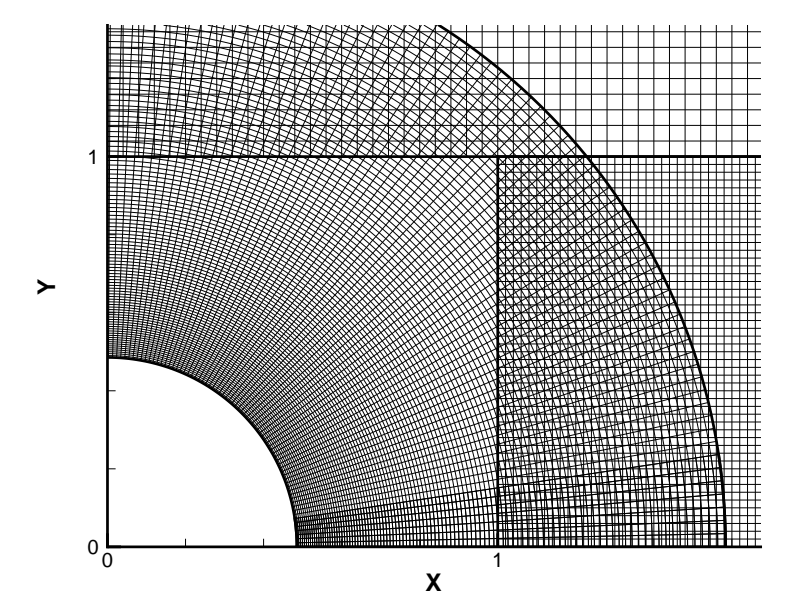


Figure 6. Overset grids

pseudo mean flow is the incoming uniform flow at all four boundaries, namely,

$$\bar{u}_p = M, \ \bar{v}_p = 0, \ \bar{\rho}_p = 1, \ \bar{p}_p = 1/\gamma$$
 (47)

with $\beta = M/(1-M^2)$. Figure 7 shows the instantaneous pressure contours at t = 5, 8, 10 and 450 calculated by direct numerical simulation (DNS), solving (1) in the physical domain and PML equations (35)-(38) in the absorbing zones. The initial transient pressure wave exits the computational domain without any noticeable reflection, followed by periodic vortex shedding. Figure 8 shows the vorticity contours at t = 450. The absorption of the non-linear vortices by the PML zone at the outflow is clearly seen.

In Figure 9, we show the v-velocity at a point close to the outflow boundary, (x, y) = (9, 0), as a function of time. Also plotted, in symbols, are the results of a reference solution computed using a larger computational domain. The reference solution is obtained using a computational domain of $[-7, 30] \times [-7, 7]$. Very good agreement is observed. Figures 7-9 indicate that the use of PML domain at the outflow causes very little reflection as the vortices convect out of the computational domain.

IV. Conclusions

A time-domain PML boundary condition for the compressible non-linear Navier-Stokes equation has been derived following a recently developed method for non-linear Euler equations. Numerical examples of a viscous vortex transport and vortex shedding from a viscous flow over a circular cylinder are presented that demonstrate the feasibility and effectiveness of proposed PML as an absorbing boundary condition for non-linear viscous flow simulations.

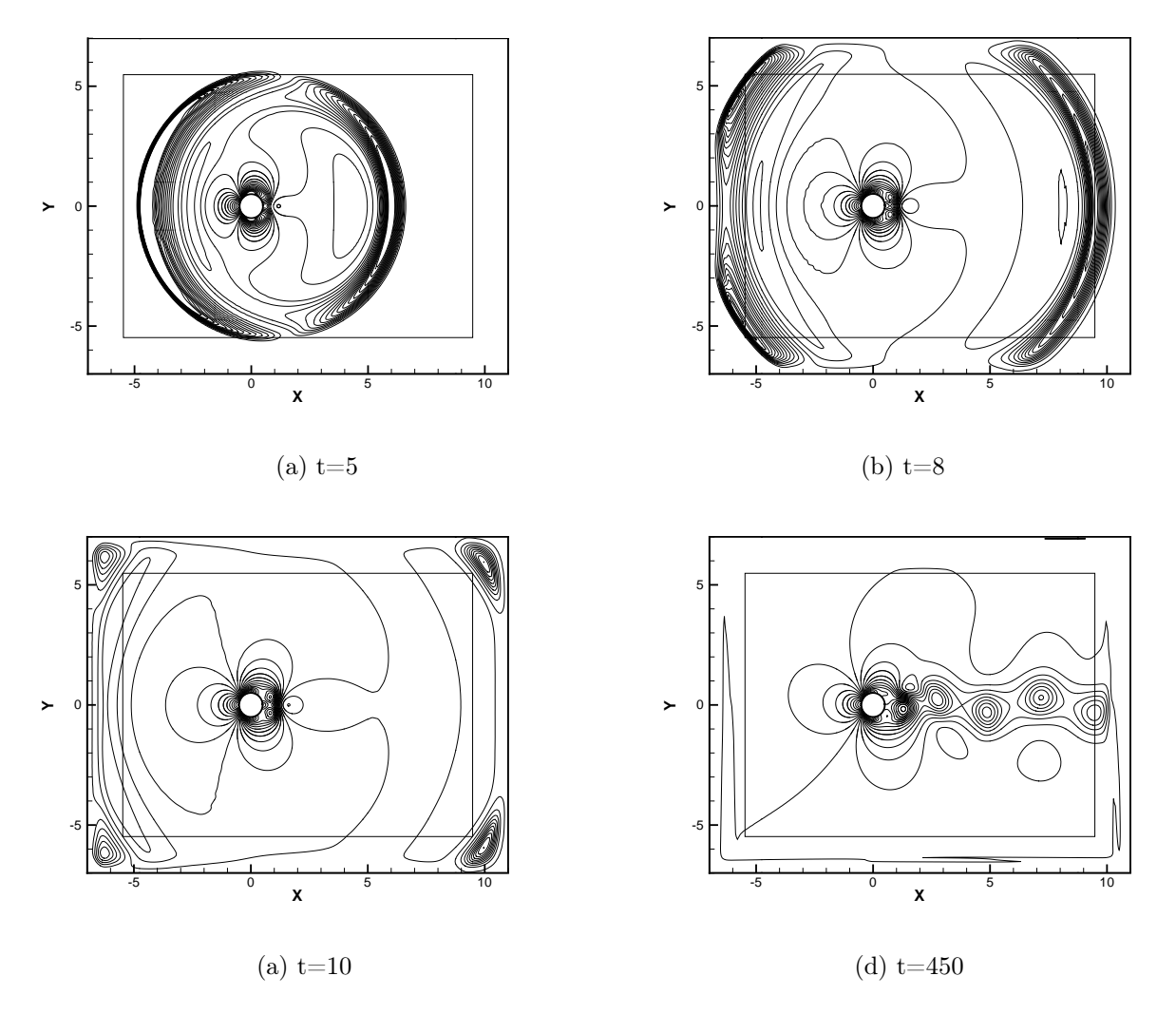


Figure 7. Pressure contour plots at time $t=5,\,t=8,\,t=10,\,t=450$

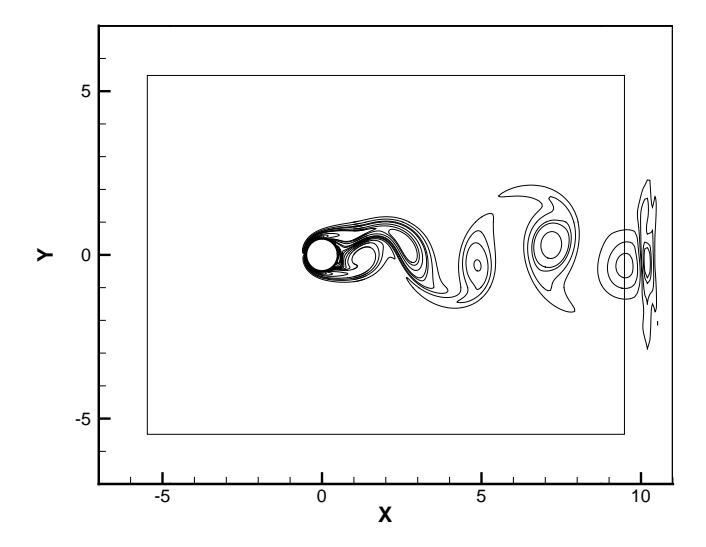


Figure 8. Vorticity contour plots at time t=450

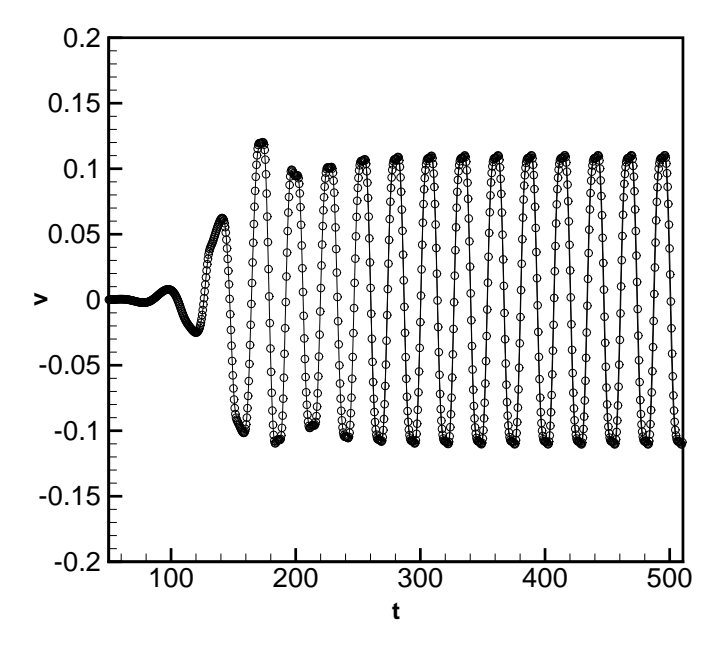


Figure 9. Comparison with large domain reference solution. Solid line: computational; circle: larger domain calculation.

ACKNOWLEDGEMENT

This work is supported by grants from the National Science Foundation DMS-0411402(F.Q. Hu), the National Science Foundation of China 10472010 and the Specialized Research Fund for the Doctoral Program of Higher Education 2005006021(X.D. Li and D. K. Lin).

References

- ¹E. Becache, A.-S. Bonnet-Ben Dhia and G. Legendre, Perfectly Matched layers for the convected Helmholtz equation, SIAM Journal on Numerical Analysis, Vol. 42, No. 1, 409-433, 2004.
- ²E. Becache, S. Fauqueux and P. Joly, Stability of perfectly matched layers, group velocities and anisotropic waves, Journal of Computational Physics, Vol. 188, 399-433, 2003.
- ³J. P. Berenger, A Perfectly Matched Layer for the Absorption of Electromagnetic waves, Journal of Computational Physics, Vol. 114, 185-200, 1994.
- ⁴T. Hagstrom and I. Nazarov, Absorbing layers and radiation boundary conditions for jet flow simulations, AIAA paper 2002-2606, 2002.
- ⁵T. Hagstrom and I. Nazarov, Perfectly matched layers and radiation boundary conditions for shear flow calculations, AIAA paper 2003-3298, 2003.
- ⁶T. Hagstrom, J. Goodrich, I. Nazarov and C. Dodson, High-order methods and boundary conditions for simulating subsonic flows, AIAA paper 2005-2869, 2005
- ⁷M. E. Hayder and H. L. Atkins, Experiences with PML boundary conditions in fluid-flow computations, IUTAM symposium of computational methods for unbounded domains, T. L. Geers (ed.), Kluwer Academic Publishers, 207-216, 1998.
- ⁸F. Q. Hu, On absorbing boundary conditions of linearized Euler equations by a perfectly matched layer, Journal of Computational Physics, Vol. 129, 201-219, 1996.
- ⁹F. Q. Hu, On Perfectly Matched Layer as an absorbing boundary condition, AIAA paper 96-1664, 1996
- ¹⁰F. Q. Hu, A stable, Perfectly Matched Layer for linearized Euler equations in unsplit physical variables, Journal of Computational Physics, Vol. 173, 455-480, 2001.
- ¹¹F. Q. Hu, A perfectly matched layer absorbing boundary condition for linearized Euler equations with a non-uniform meanflow, Journal of Computational Physics, Vol. 208, 469-492, 2005.
- ¹²F. Q. Hu, On the construction of PML absorbing boundary condition for the non-linear Euler equations, AIAA paper 2006-0798, 2006.
- ¹³F. Q. Hu, Development of PML absorbing boundary condition for Computational Aeroacoustics: A progress review, to appear in Computers & Fluids, 2006.
- ¹⁴F. Q. Hu, M. Y. Hussaini and J. L. Manthey, Low-dissipation and -dispersion Runge-Kutta schemes for computational acoustics", Journal of Computational Physics, Vol. 124, 177-191, 1996.
- ¹⁵X.D. Li and J.H. Gao, Numerical Simulation of the generation mechanism of axisymmetric supersonic jet screech tones, Physics of Fluids, Vol.17, Art No: 085105, 2005.
- ¹⁶X.D. Li and J.H. Gao, Numerical Simulation of Three-Dimensional supersonic jet screech tones, AIAA paper 2005-2882, 2005.
- ¹⁷P. G. Petropoulos, Reflectionless sponge layers as absorbing boundary conditions for numerical simulation of Maxwell's equations in rectangular, cylindrical and spherical coordinates, SIAM J. App. Math., Vol. 60, 1037-1058, 2000.
- ¹⁸C. K. W. Tam and J. C. Webb, Dispersion-relation-preserving schemes for computational acoustics, Journal of Computational Physics, Vol. 107, 262-281, 1993.
- ¹⁹L. Zhao and A. C. Cangellaris, GT-PML: Generalized theory of Perfectly Matched Layers and its application to the reflectionless truncation of finite-difference time-domain grids, IEEE Trans. Microwave Theory Tech., Vol. 44, 2555-2563, 1996.